Deposited the gate insulator

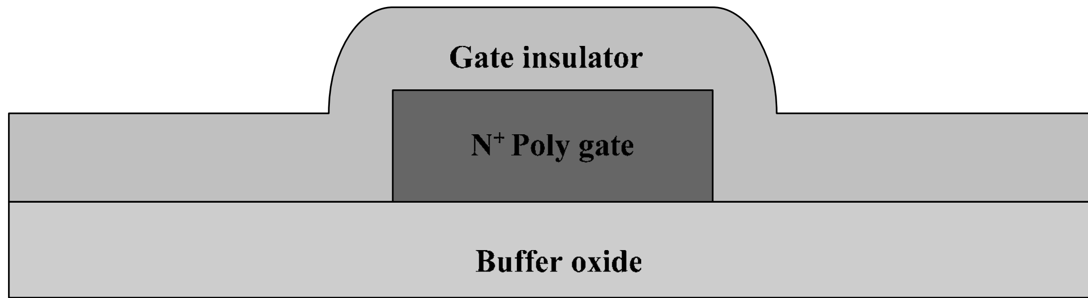

Deposited the a-Si channel

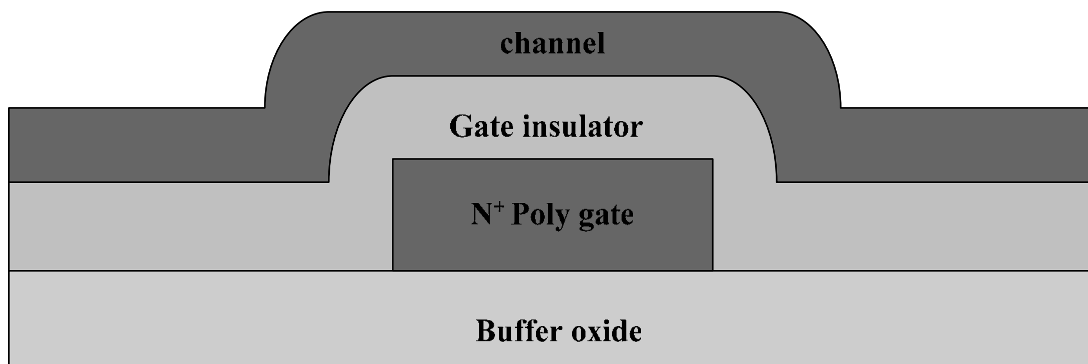

Ion implantation; B^{11} 15KeV 1E16

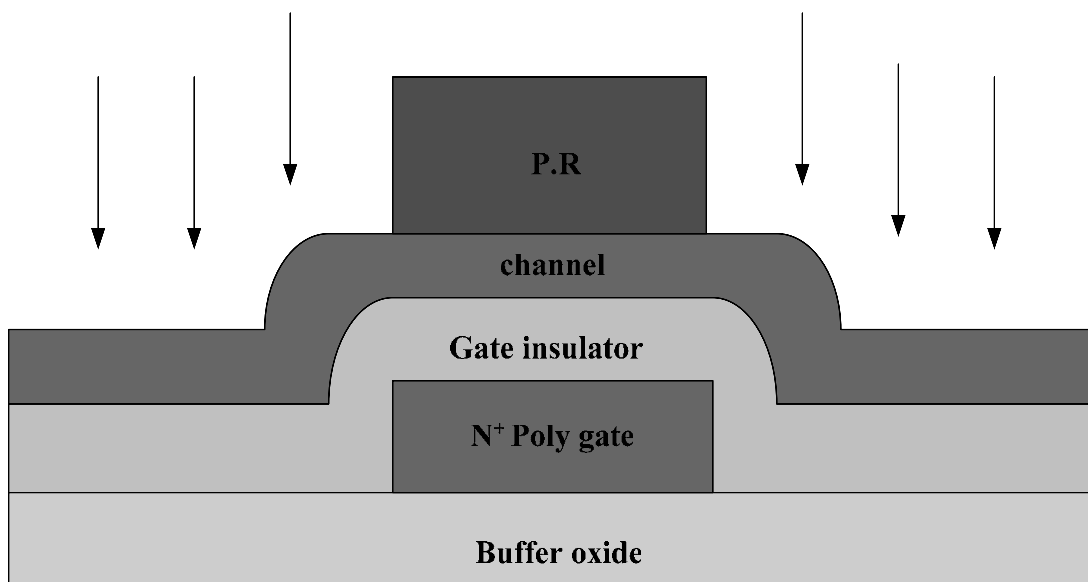

Figure 2.1 Process flows of p-type bottom-gate poly-Si TFTs.

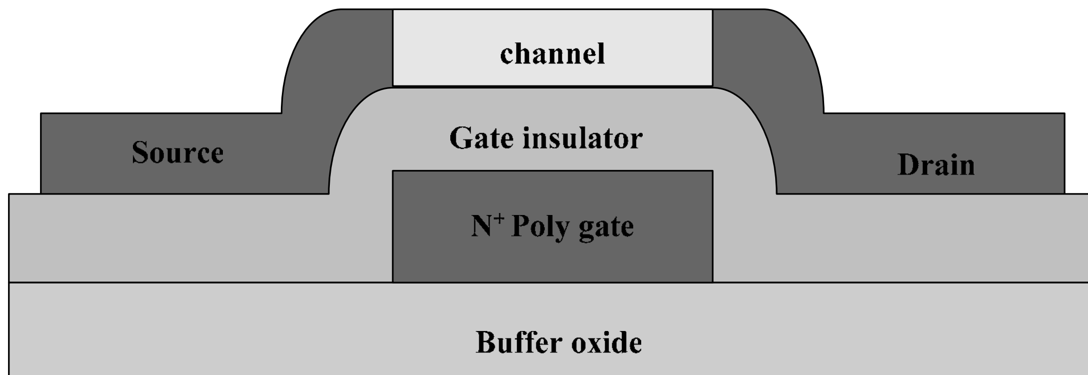

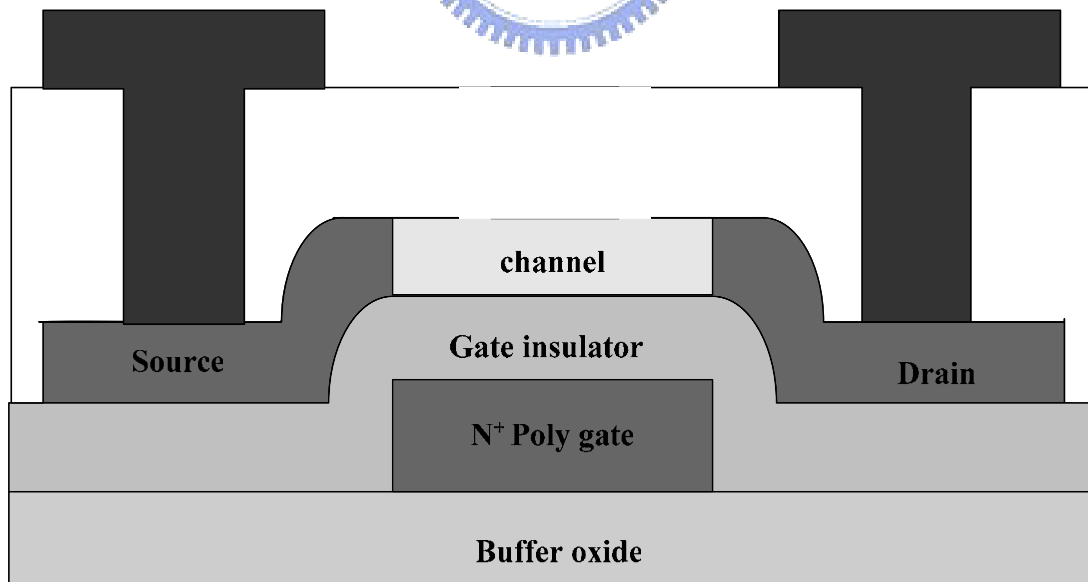

Figure 2.1 Process flows of p-type bottom-gate poly-Si TFTs.

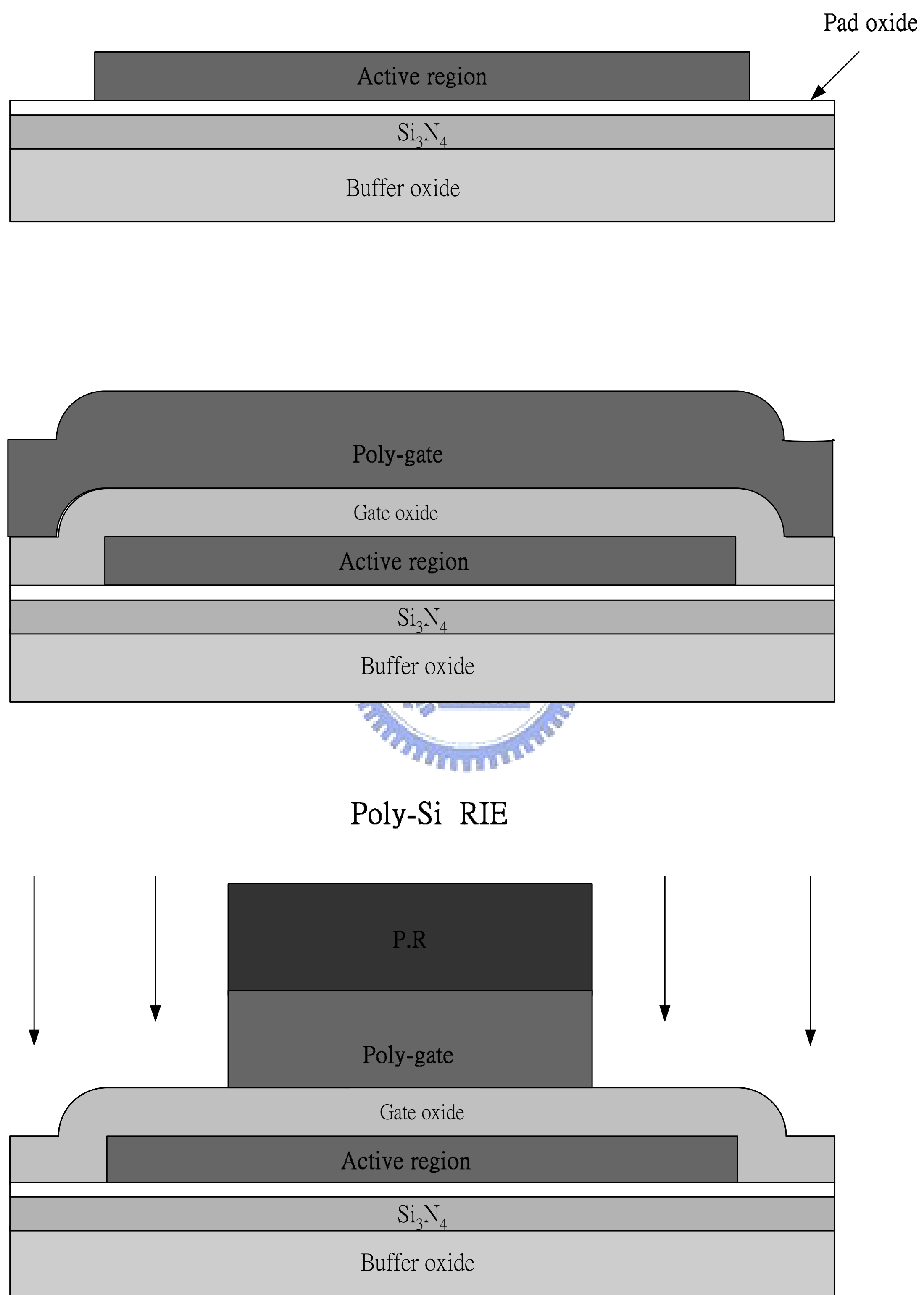

Figure 2.2 Process flows of n-type buffer nitride layer poly-Si TFTs

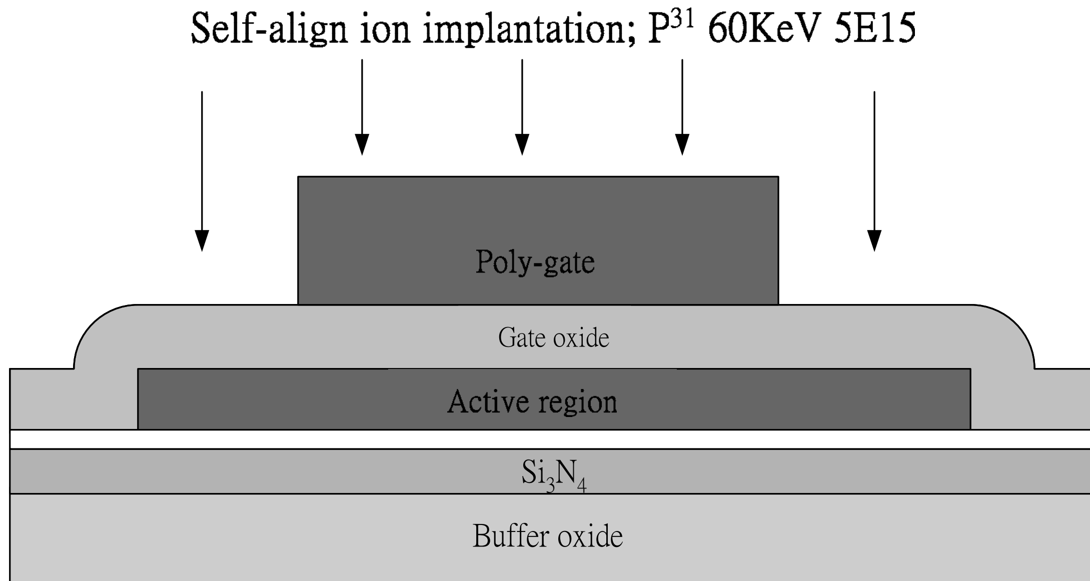

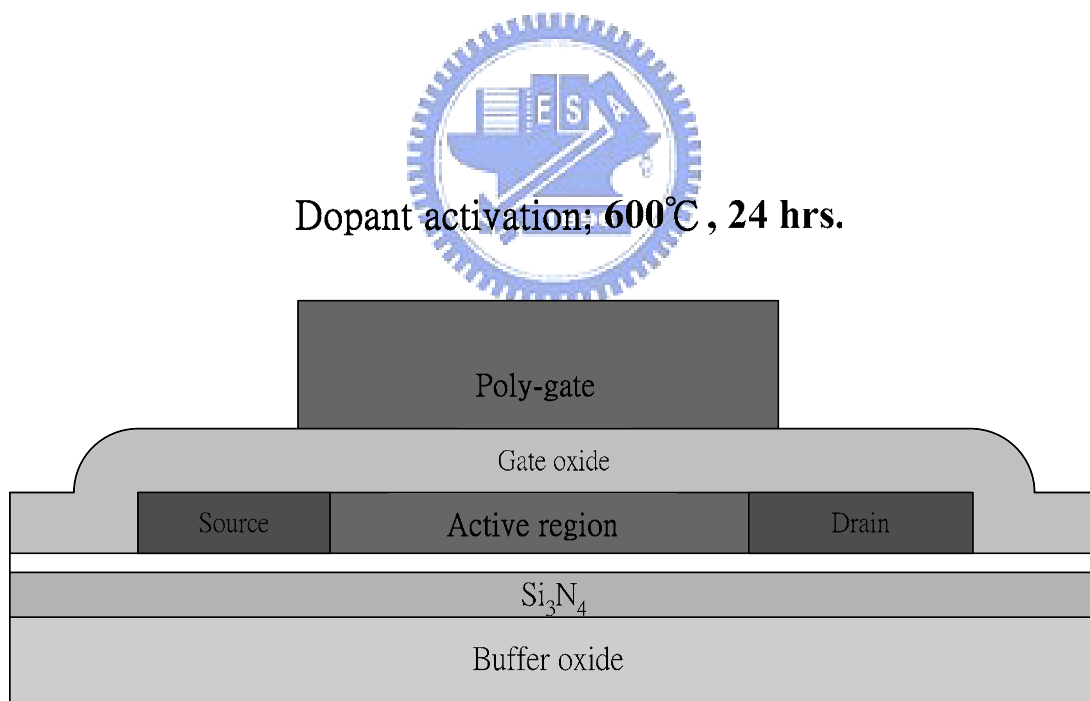

Figure 2.2 Process flows of n-type buffer nitride layer poly-Si TFTs

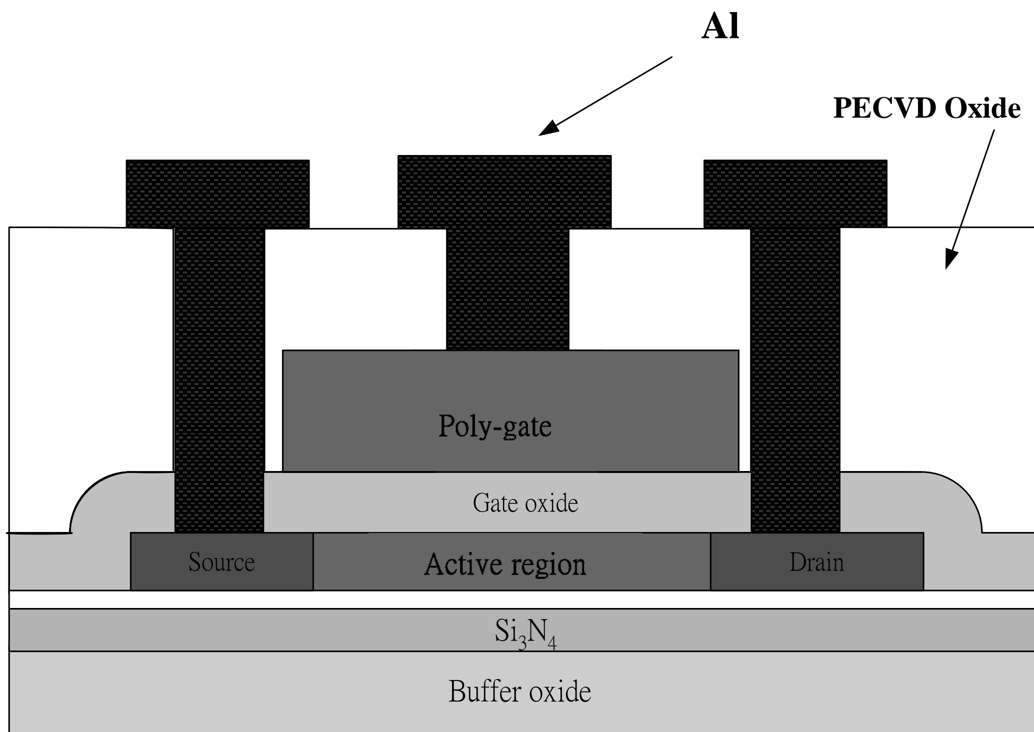

Figure 2.2 Process flows of n-type buffer nitride layer poly-Si TFTs.

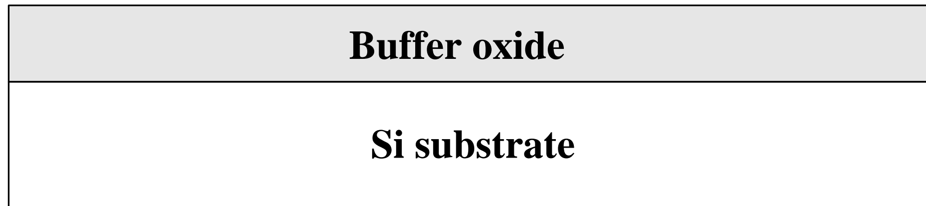

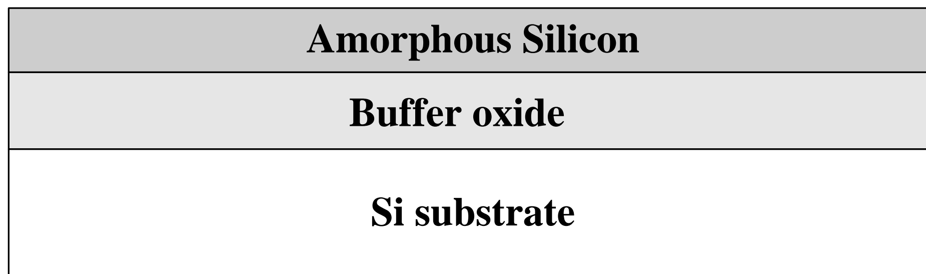

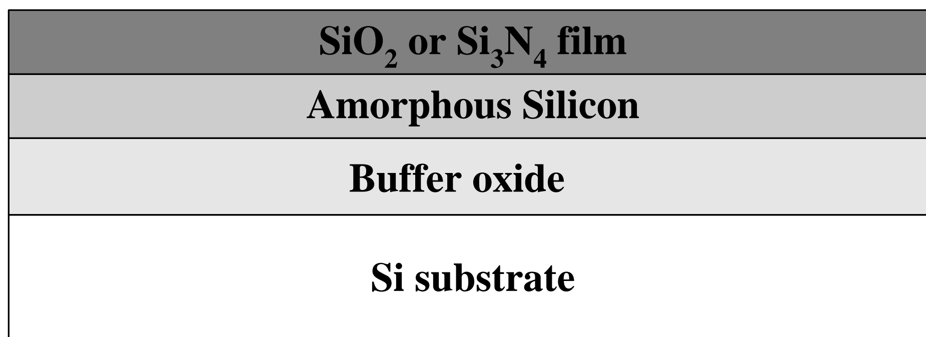

Figure 2.3 Process flows of SIMS analysis sample

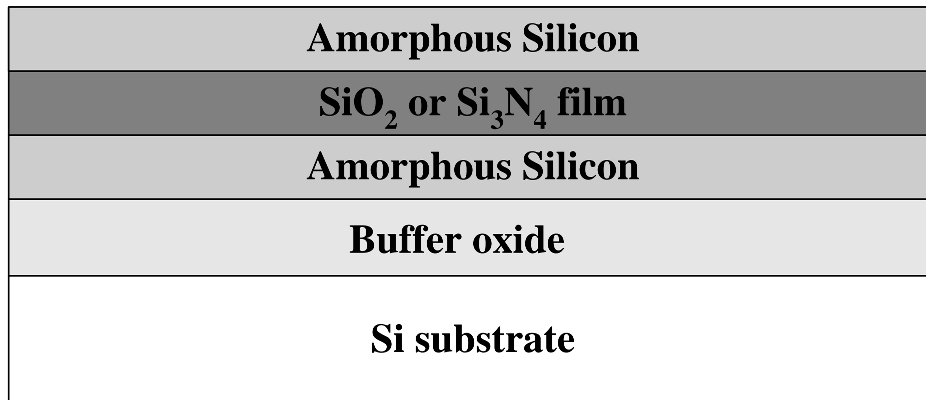

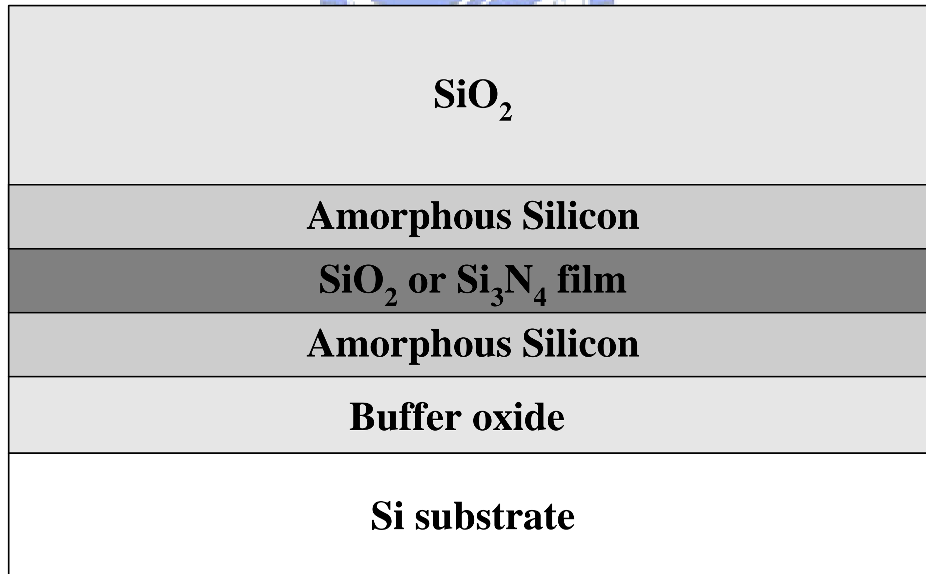

Figure 2.3 Process flows of SIMS analysis sample

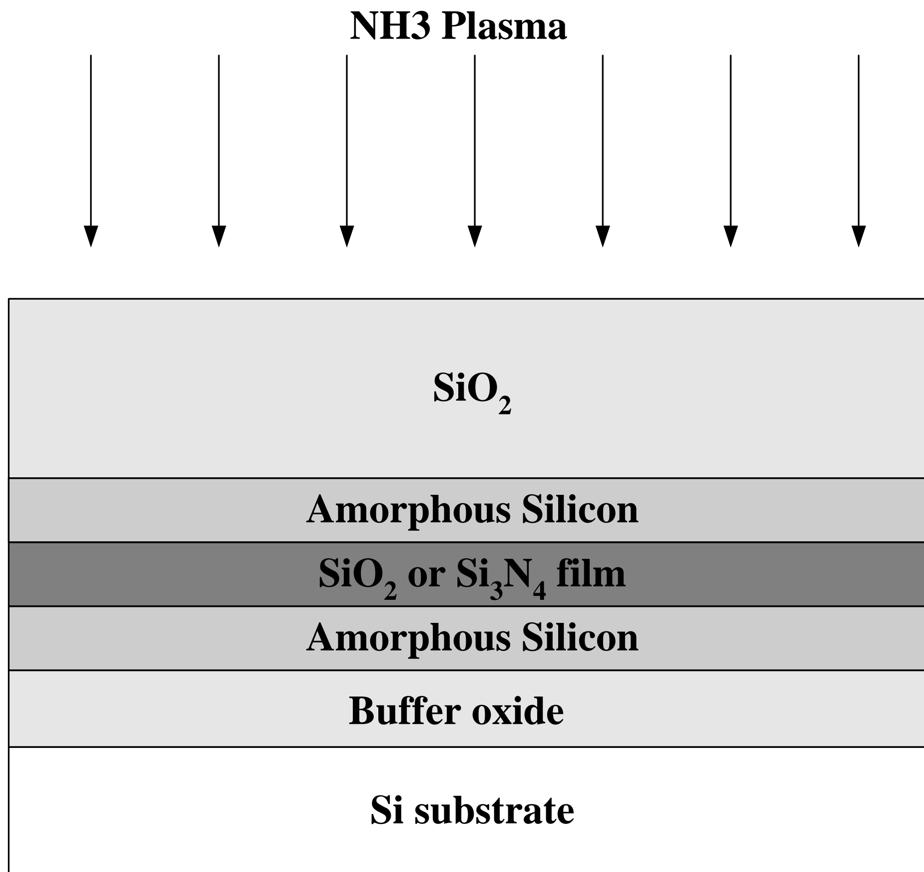

Remove passivation oxide

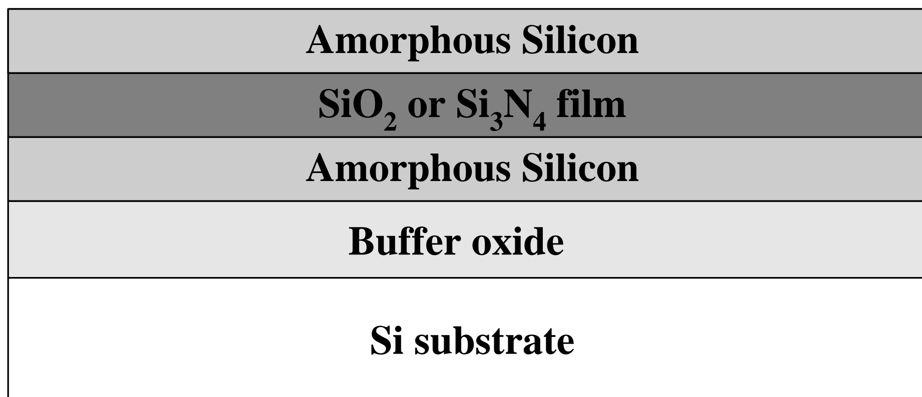

Figure 2.3 Process flows of SIMS analysis sample

Sample	Gate insulator	V_{th} (V)	Mobility (cm^2/V-s)	SS (mV/dec)	I_{on} (A)	I_{off} (A)	I_{on}/I_{off}
Sample A before hydrogenation	SiO_2	-23.6	2.4	1916	8.1E-6	2.6E-10	3.12E+4
Sample A after 360min hydrogenation	SiO_2	-8.64	9.3	334	2.28E-4	1.9E-13	1.2E+9
Sample B before hydrogenation	Si_3N_4	-27.3	0.1	1832	4.19E-7	1.96E-10	2.13E+3
Sample B after 300min hydrogenation	Si_3N_4	-9.3	2.1	242	5.15E-5	1.5E-13	3.43E+8

Table 2.1 The electrical characteristics of bottom-gated poly-Si TFTs before and after NH_3 plasma hydrogenation.

Sample	V_{th} (V)	Mobility (cm^2/V-s)	SS (mV/dec)	I_{on} (A)	I_{off} (A)	I_{on}/I_{off}
CTFT before hydrogenation	9.36	26.48	1860	7.67E-5	4.23E-11	1.81E+6
CTFT after 540min hydrogenation	1.22	39.86	984	3.38E-4	1.95E-11	1.77E+7
BNTFT before hydrogenation	9.36	23.29	1888	7.47E-5	5.07E-11	1.47E+6
BNTFT after 540min hydrogenation	1.22	44.84	969	3.7E-4	2.32E-11	1.6E+7

Table 2.2 The electrical characteristics of Top-gate poly-Si TFTs before and after NH_3 plasma hydrogenation.

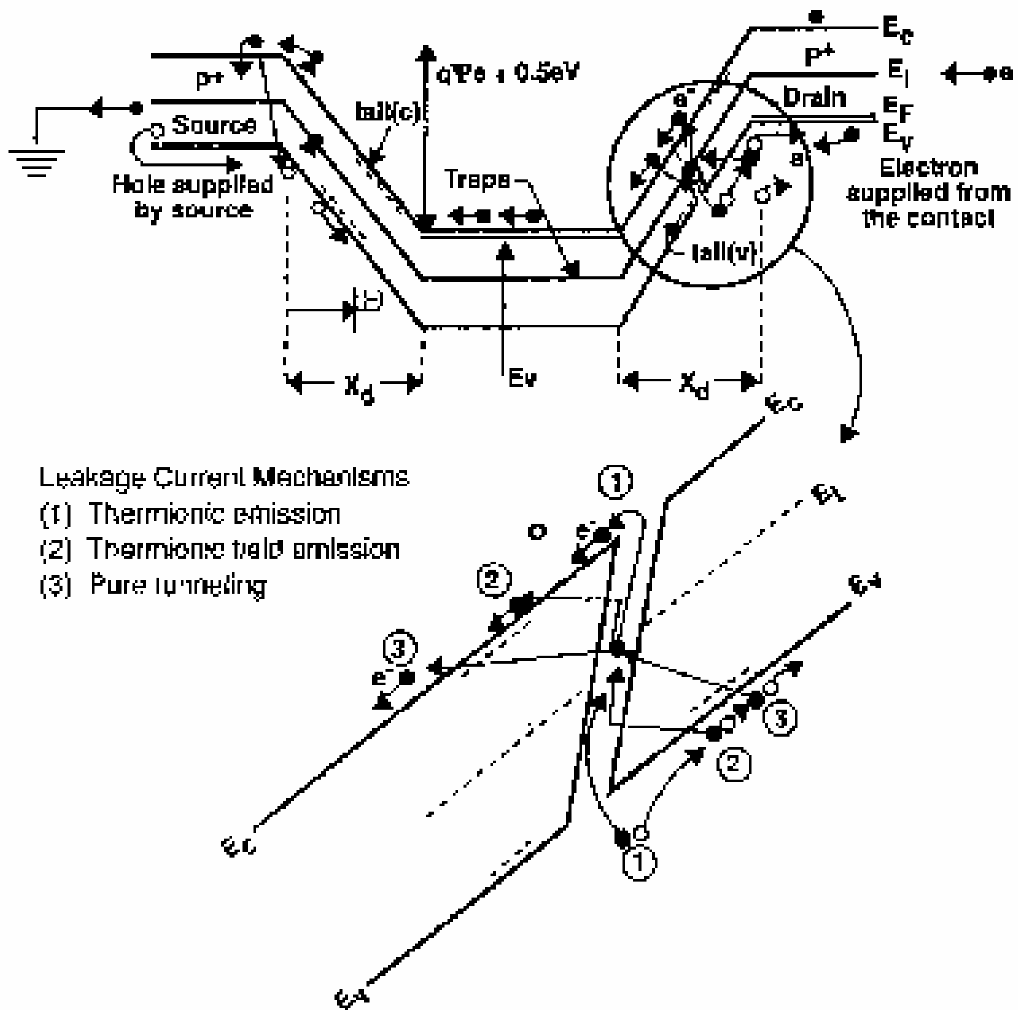

Figure 2.4 Schematic illustration of the leakage current model in poly-Si TFTs.

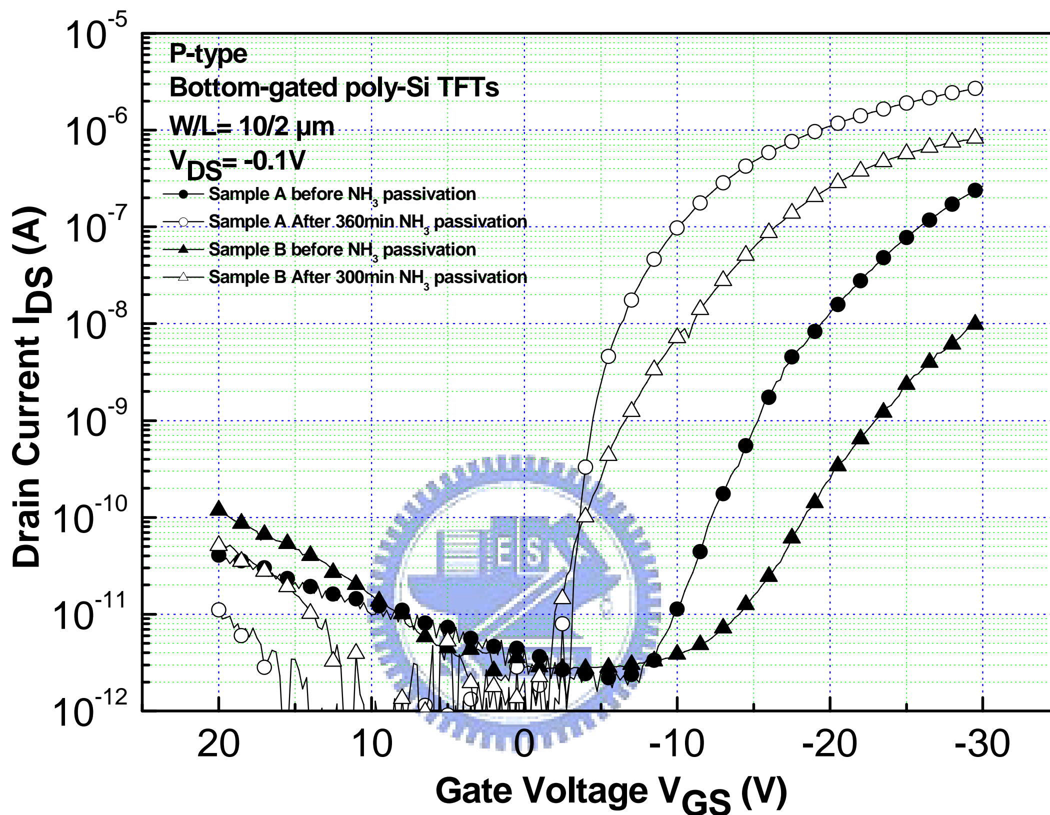

Figure 2.5 (a) Transfer characteristics for comparison of p-type bottom-gated TFTs before and after hydrogenation at V_{DS}= -0.1 V. Sample A (gate oxide), and B (gate nitride) treat 360 min, and 300min NH_3 plasma passivation.

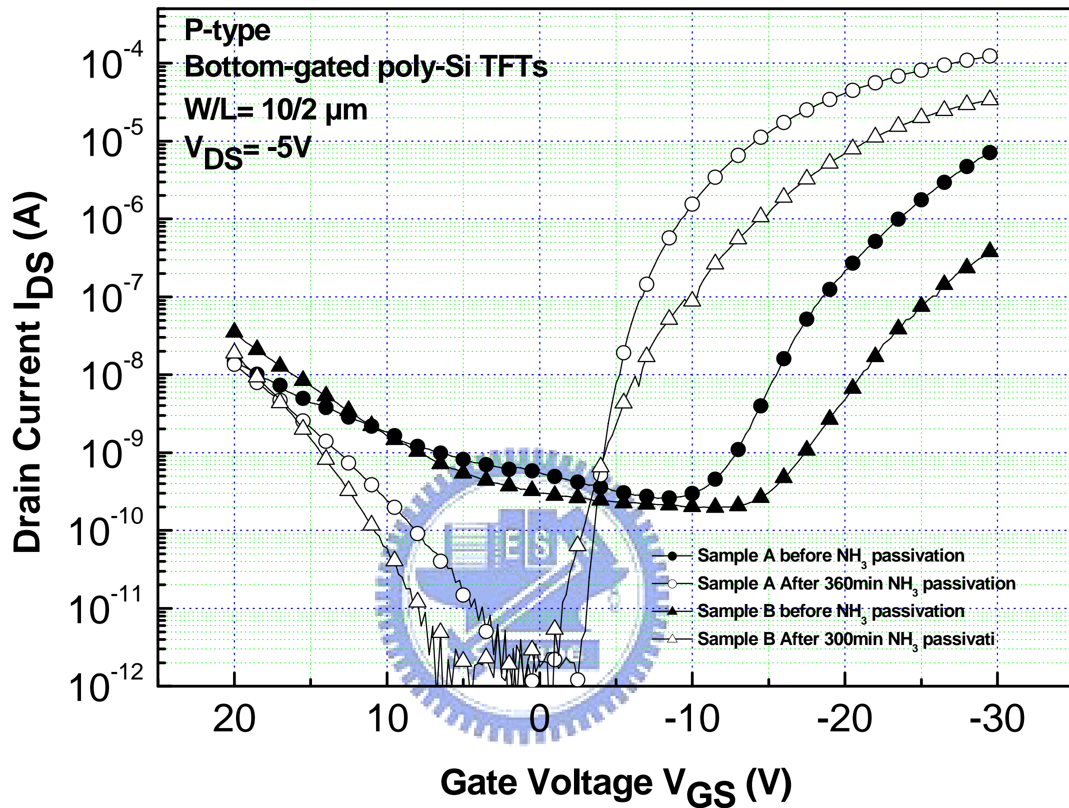

Figure 2.5 (b) Transfer characteristics for comparison of p-type bottom-gated TFTs before and after hydrogenation at V_{DS}= -5 V. Sample A (gate oxide), and B (gate nitride) treat 360 min, and 300min NH_3 plasma passivation.

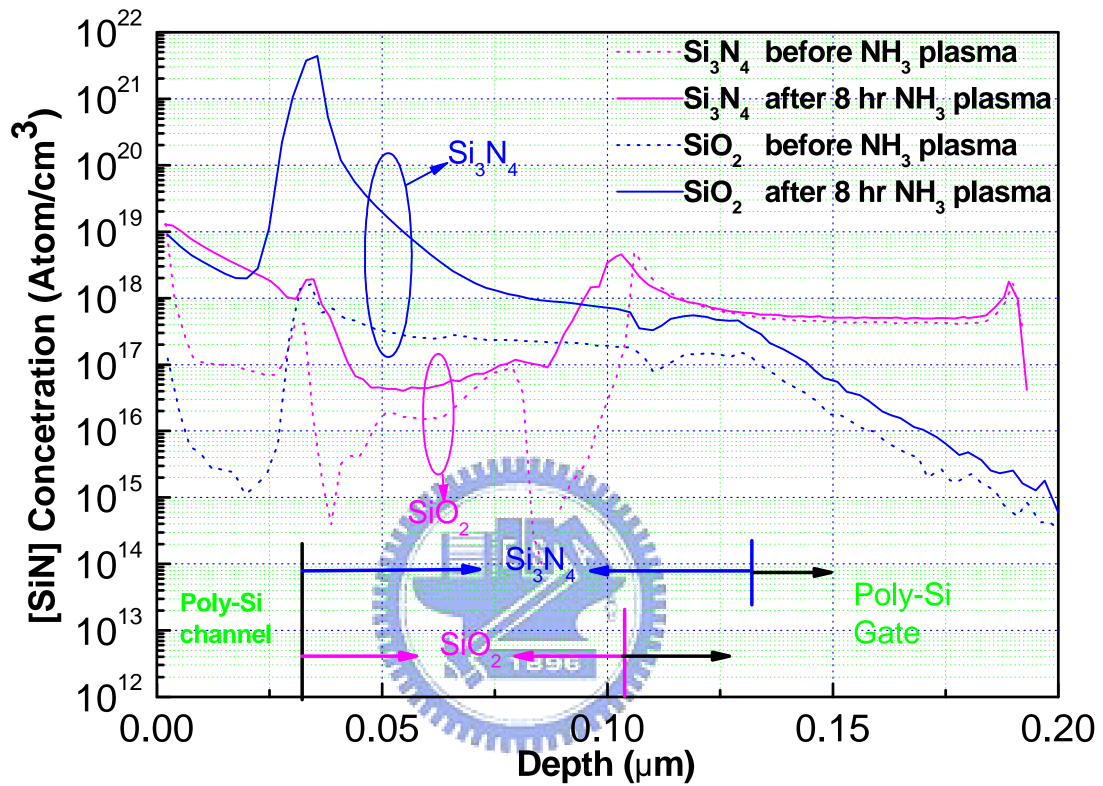

Figure 2.6 (a) The SIMS profiles of SiN for SiO_2 and Si_3N_4 with 480 min NH_3 plasma treatment.

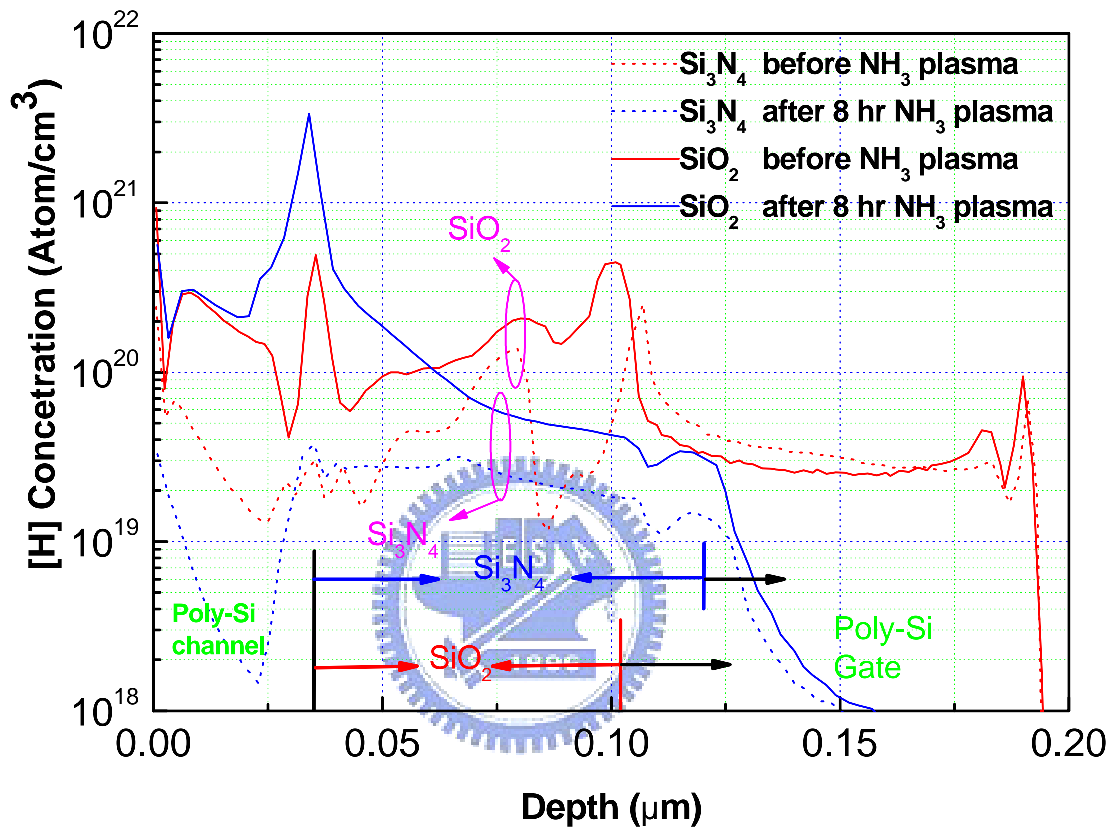

Figure 2.6 (b) The SIMS profiles of hydrogen concentration for SiO_2 and Si_3N_4 with 480 min NH_3 plasma treatment.

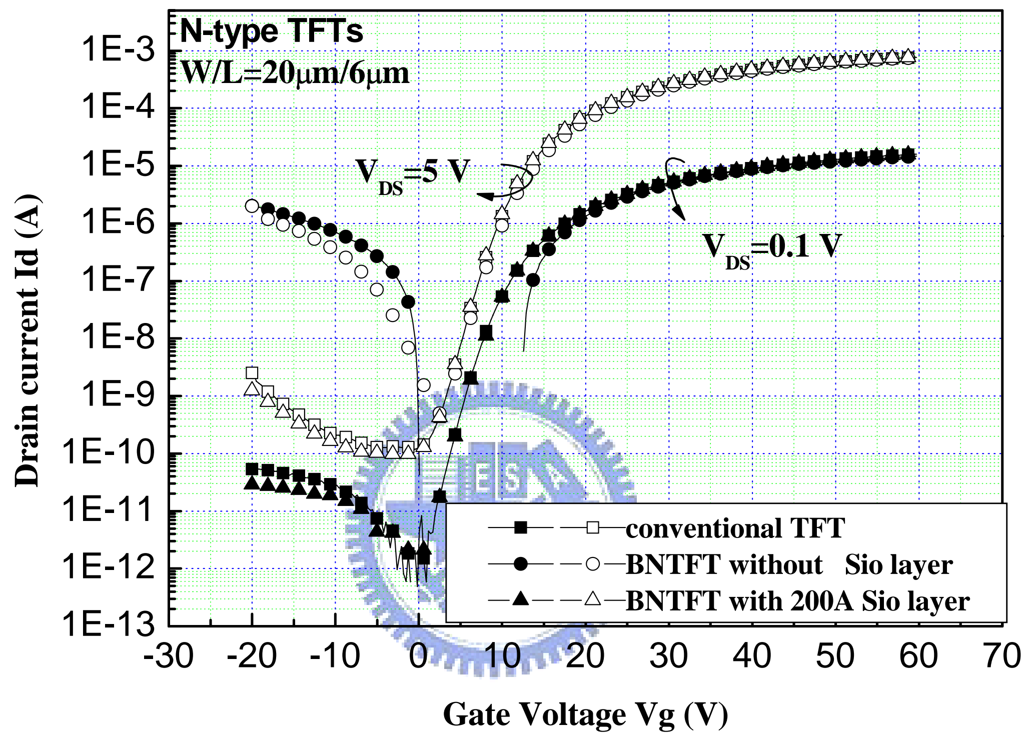

Figure 2.7 (a) Transfer characteristics for comparison of BNTFTs with and Without SiO layer at V_{DS} = 0.1V and 5V, respectively.

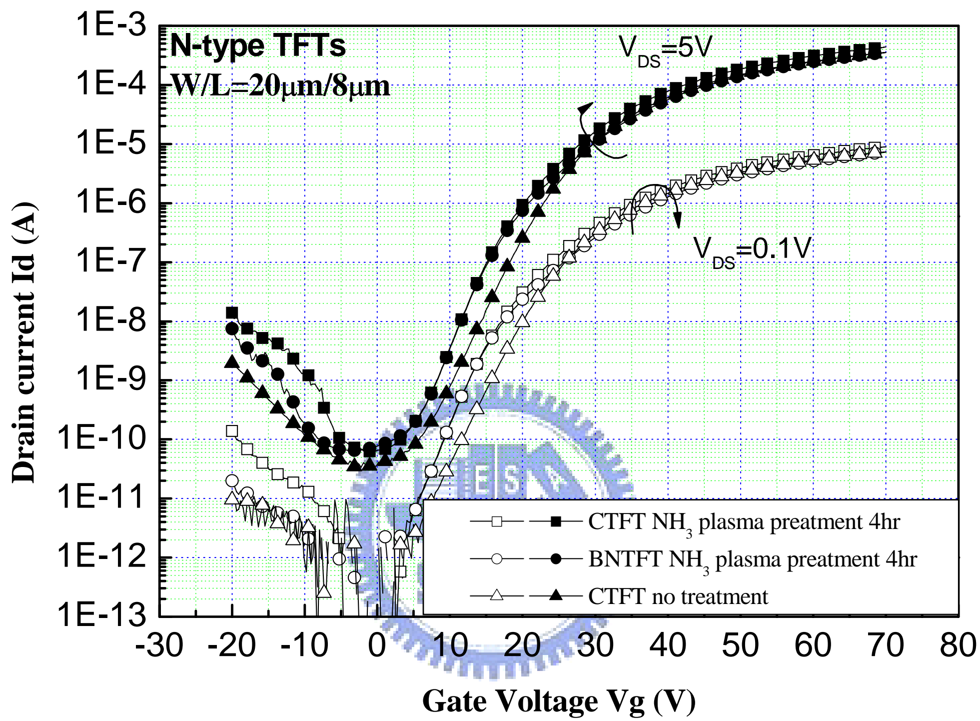

Figure 2.7 (b) Transfer characteristics for comparison of BNTFTs and CTFT pretreatment effect..

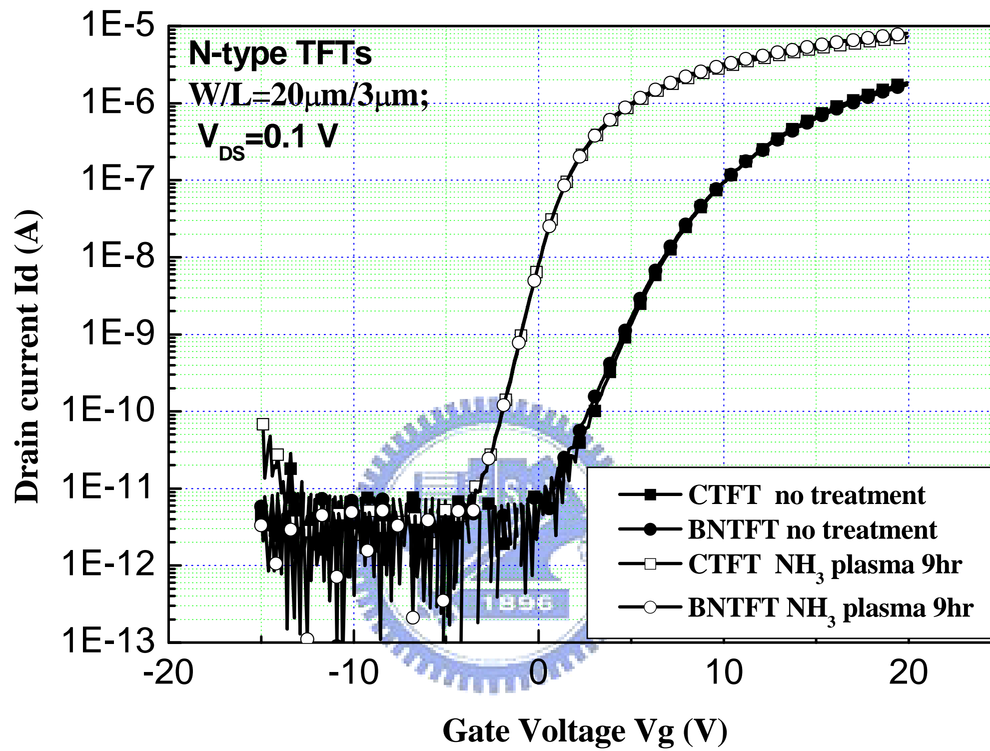

Figure 2.8 (a) Transfer characteristics for comparison of BNTFTs and CTFT before and after hydrogenation at V_{DS}= 0.1 V.

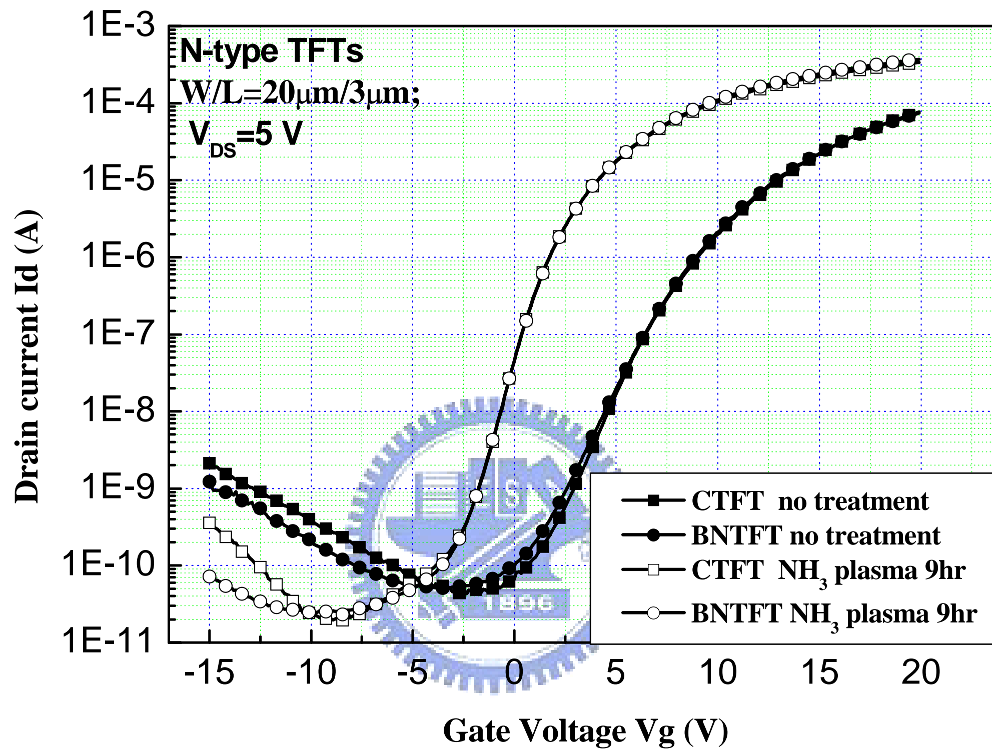

Figure 2.8 (b) Transfer characteristics for comparison of BNTFTs and CTFT before and after hydrogenation at V_{DS}= 5 V.

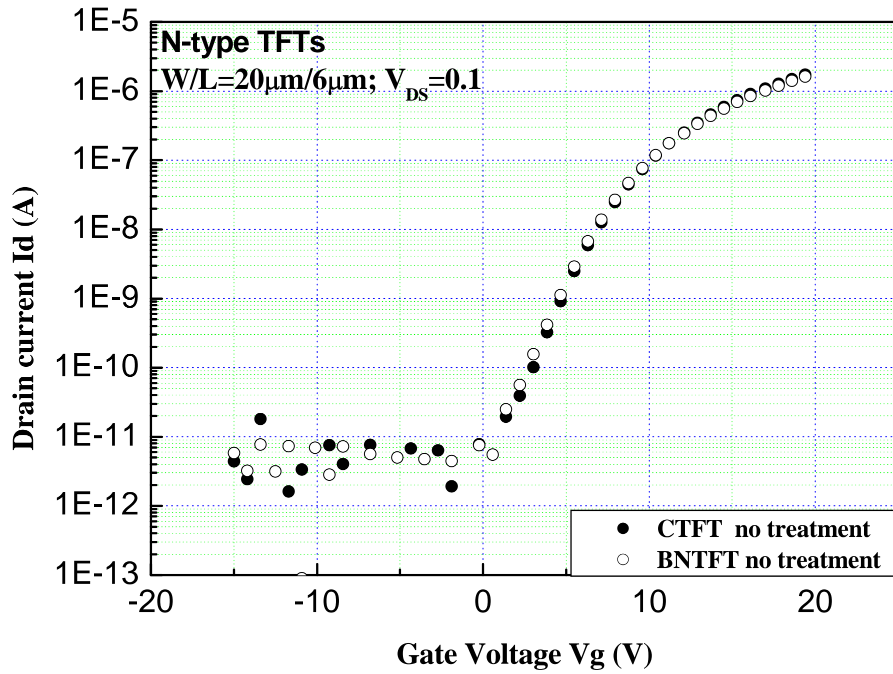

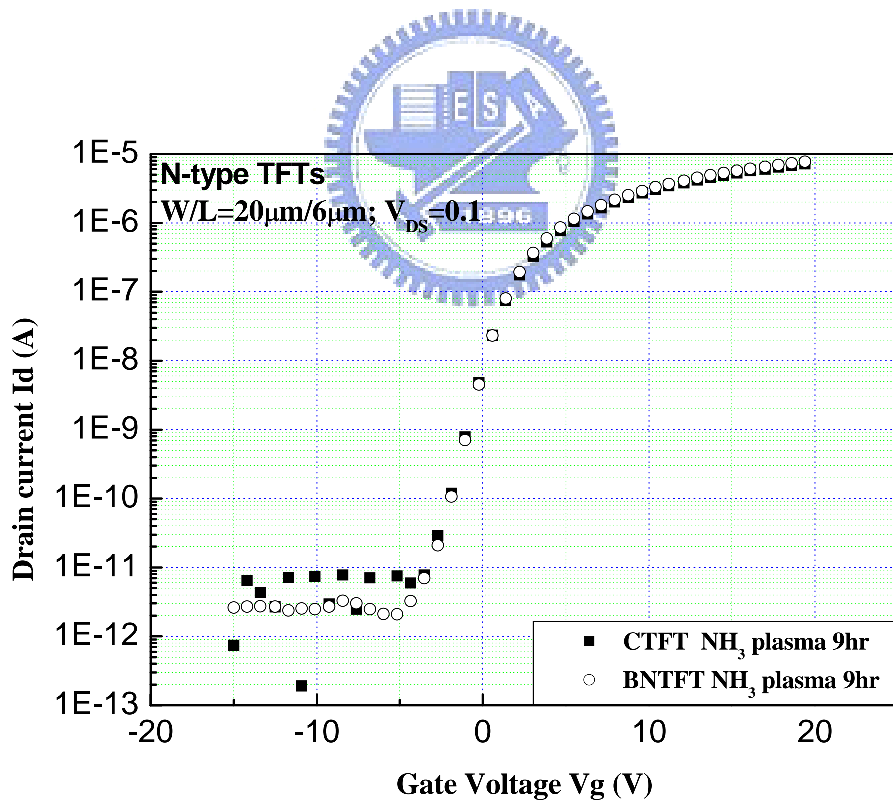

Figure 2.9 Transfer characteristics for comparison of NBTFTs and CTFT (a) before and (b) after hydrogenation at V_{DS}= 0.1 V.

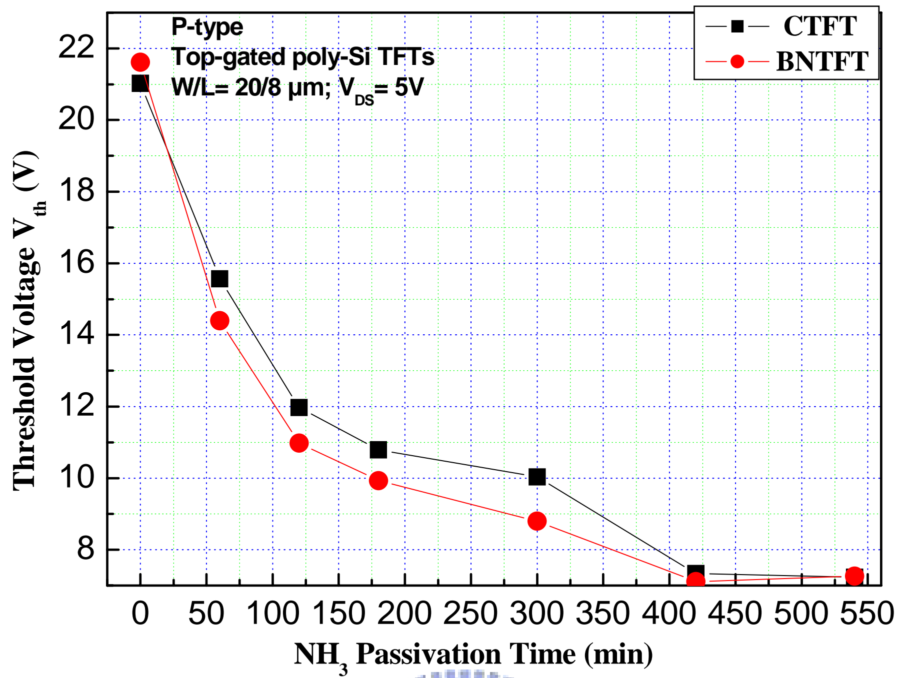

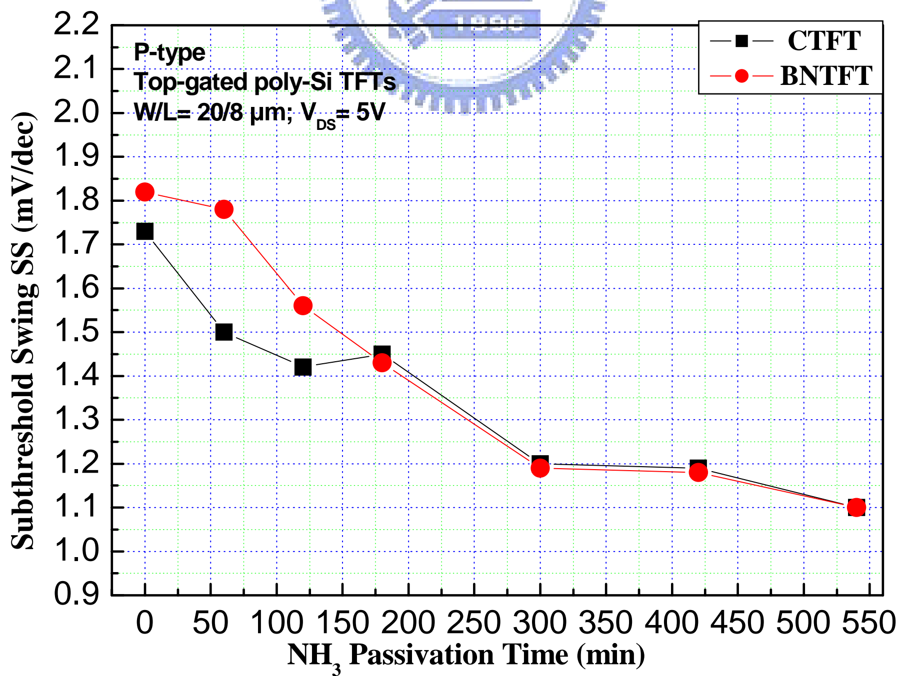

Figure 2.10 (a) Threshold voltage, and (b) Subthreshold swing as function of NH3 plasma passivation time for W = 20 μm and L = 8 μm BNTFTs.

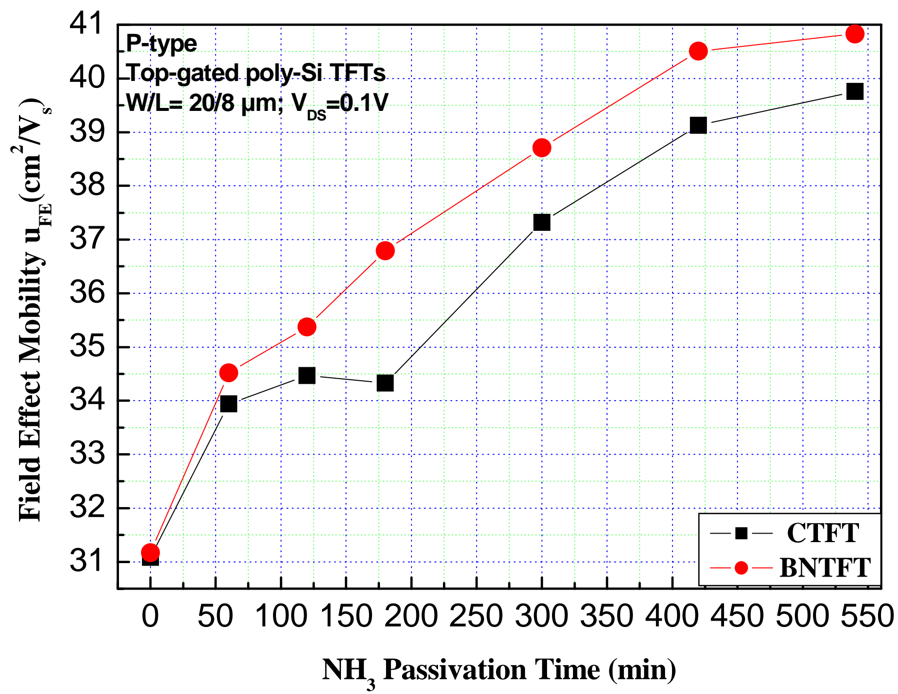

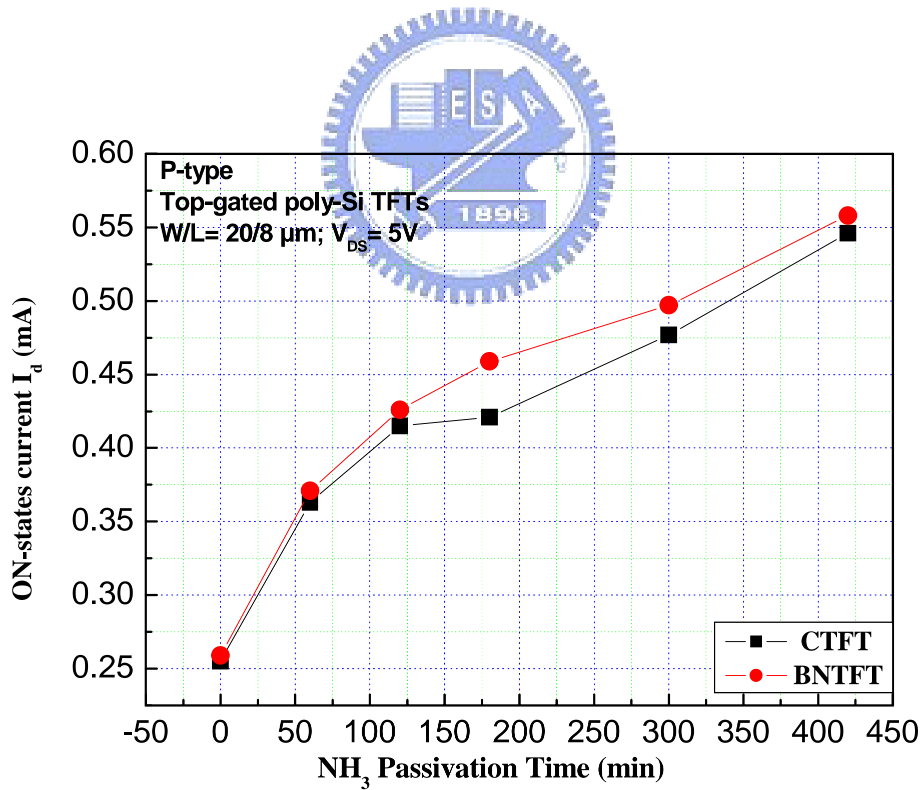

Figure 2.11 (a) Field effect mobility, and (b) ON-state current as function of NH3 plasma passivation time for W = 20 μm and L = 8 μm NBTFTs.

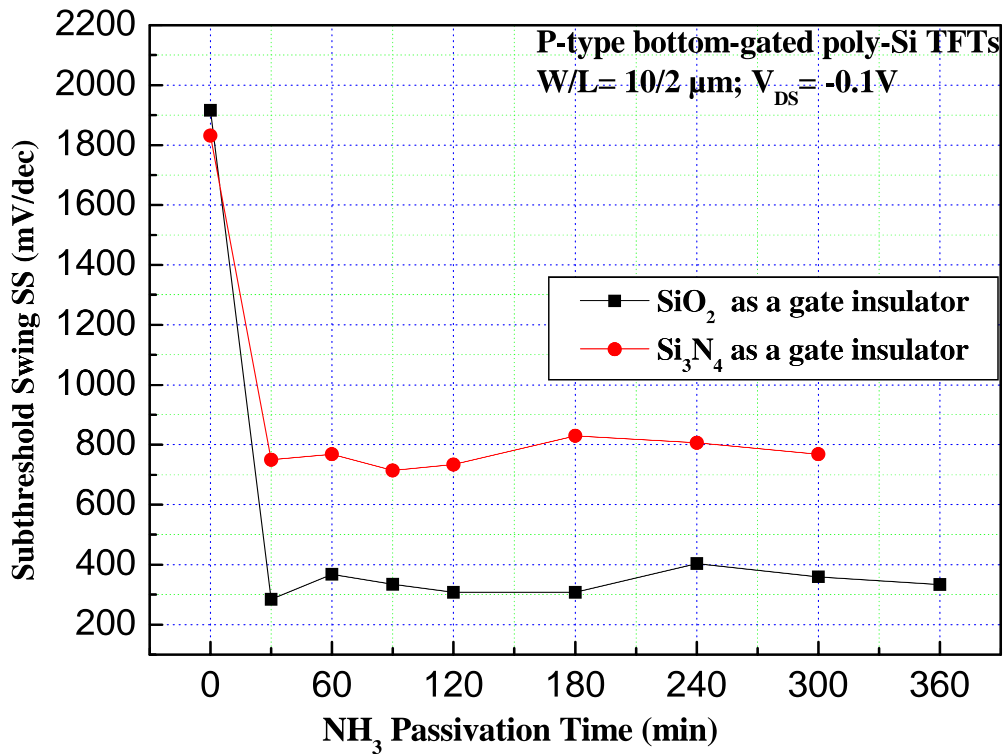

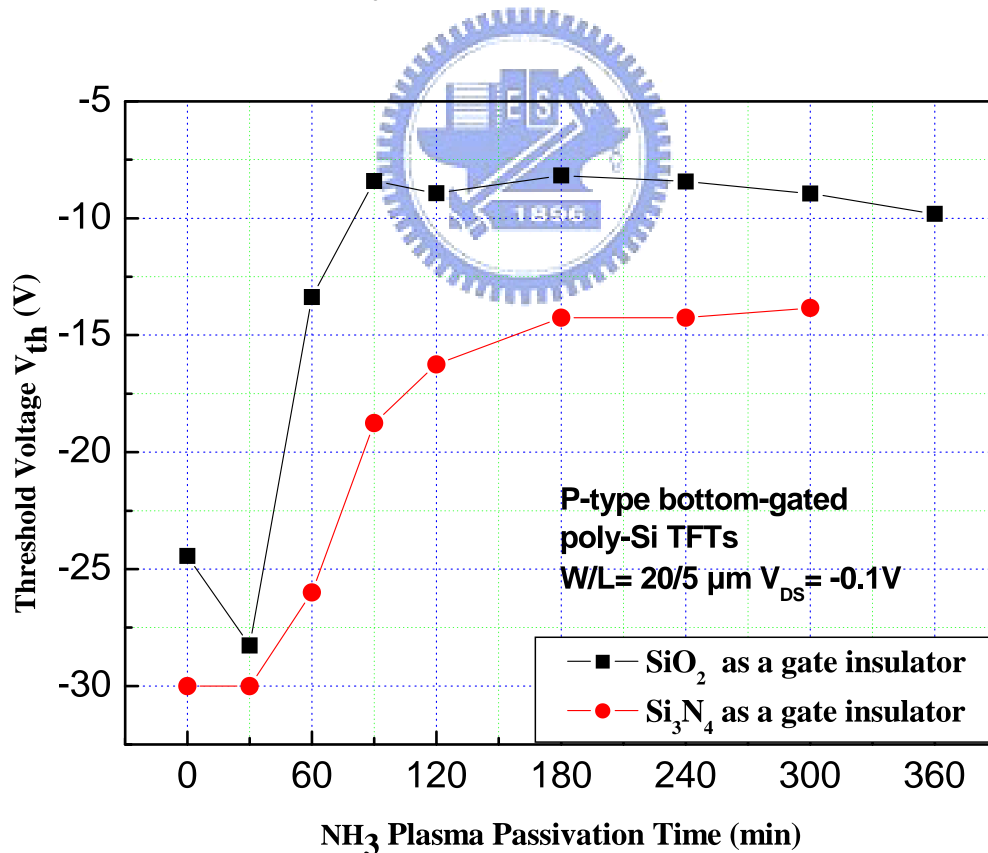

Figure 2.12 (a) Subthreshold swing, and (b) Threshold voltage as function of NH3 plasma passivation time for W = 20 μm and L = 2,5 μm p-type bottom-gate TFTs.

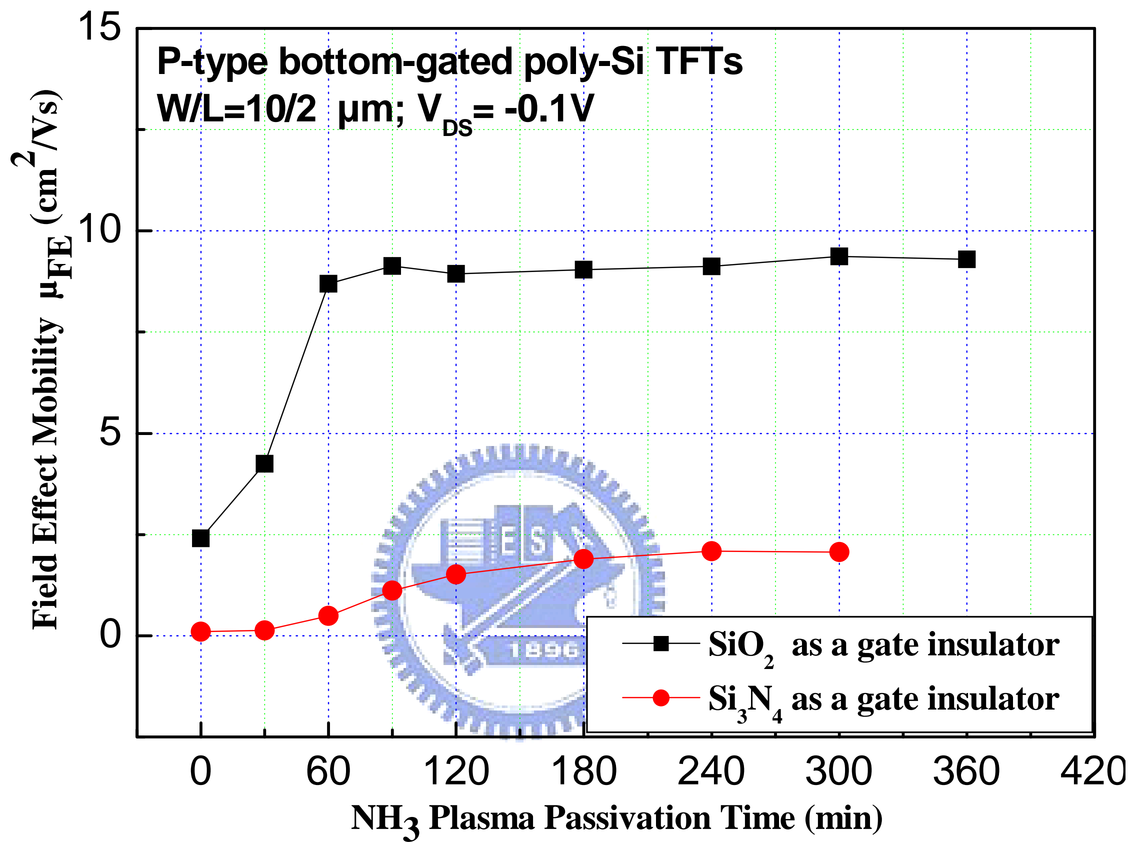

Figure 2.13 Field effect mobility as function of NH3 plasma passivation time for W = 20 μm and L = 2 μm p-type bottom-gate TFTs.

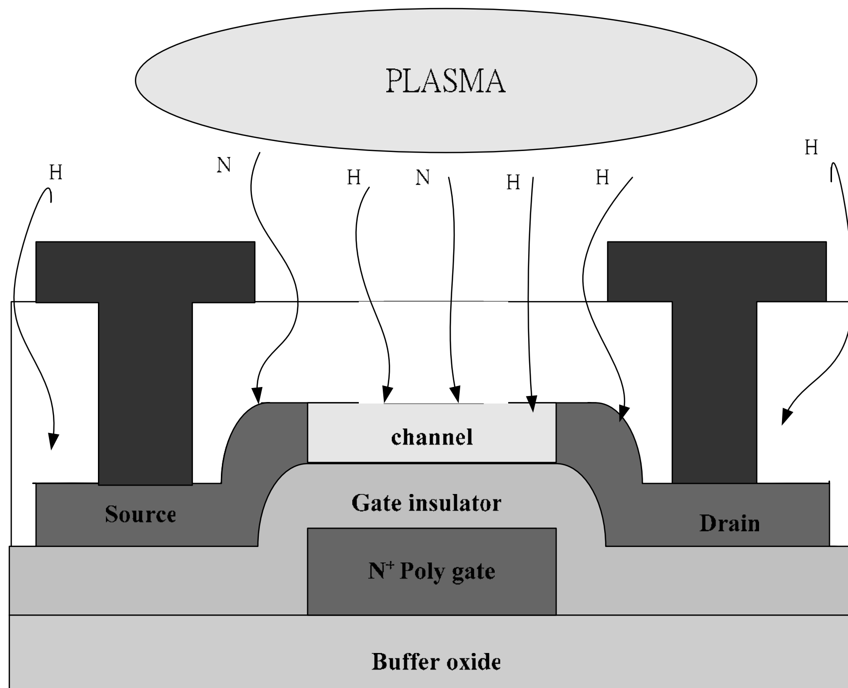

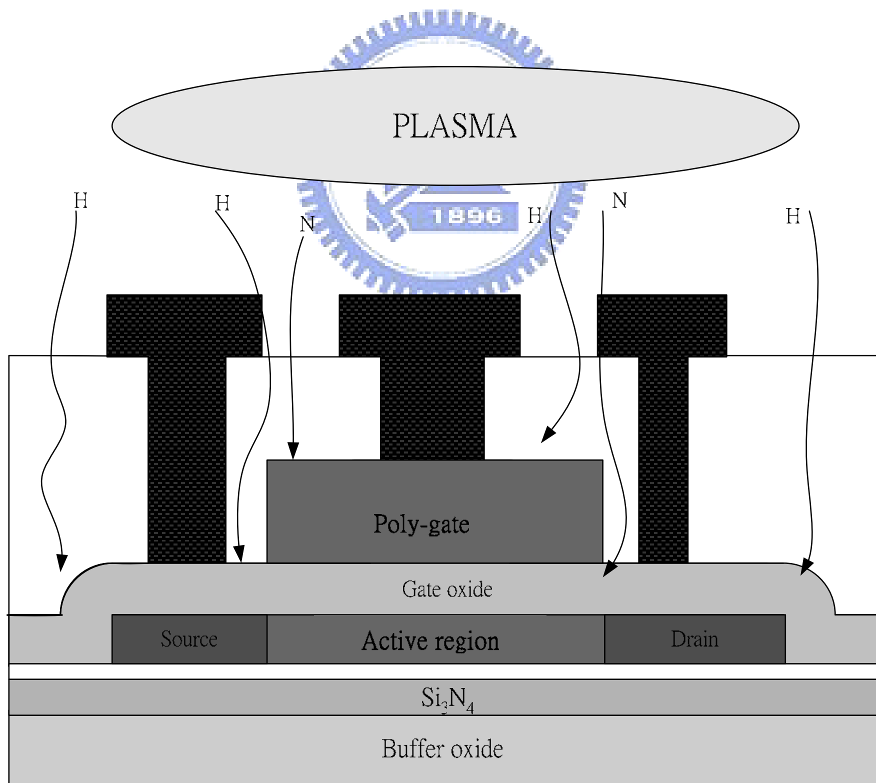

Figure 2.14 The pathway for hydrogen migration from a gaseous source to the active channel region of a (a) bottom-gate TFT and (b) top-gate BNTFT.

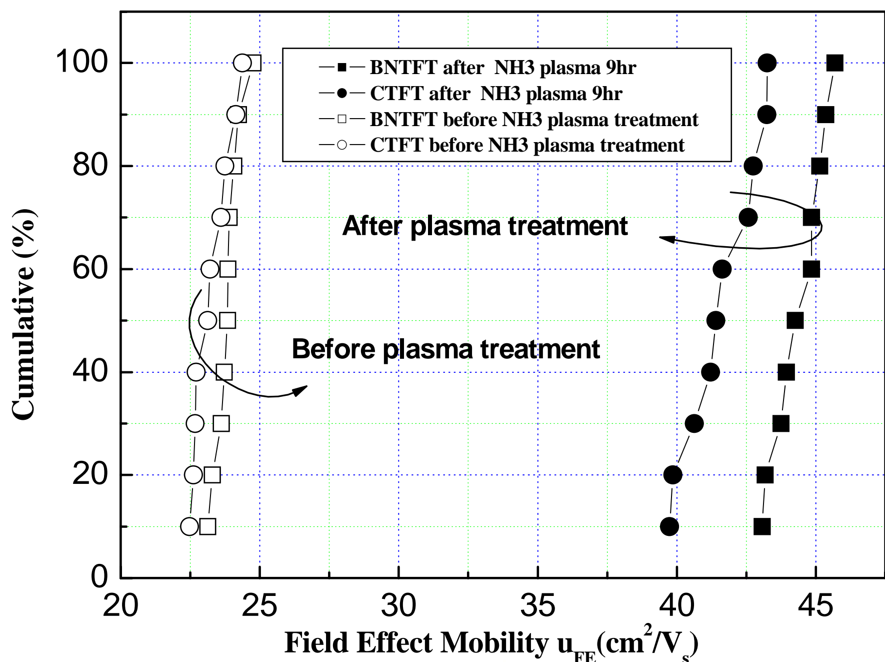

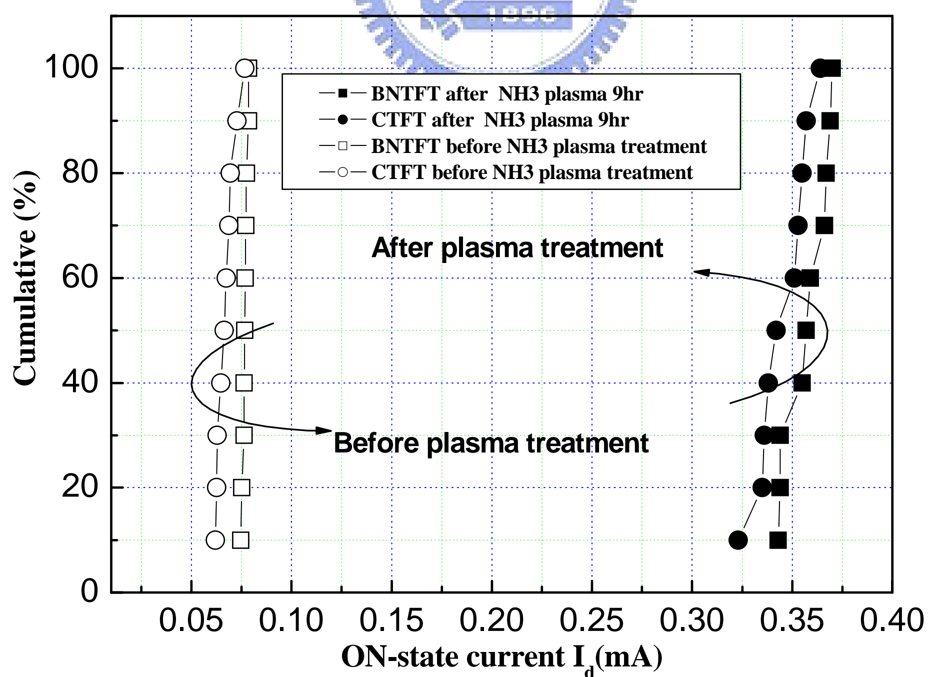

Figure 2.15 Cumulative distribution of (a) Field effect mobility (b) ON-state current before and after plasma treatment for CTFTs and BNTFTs.

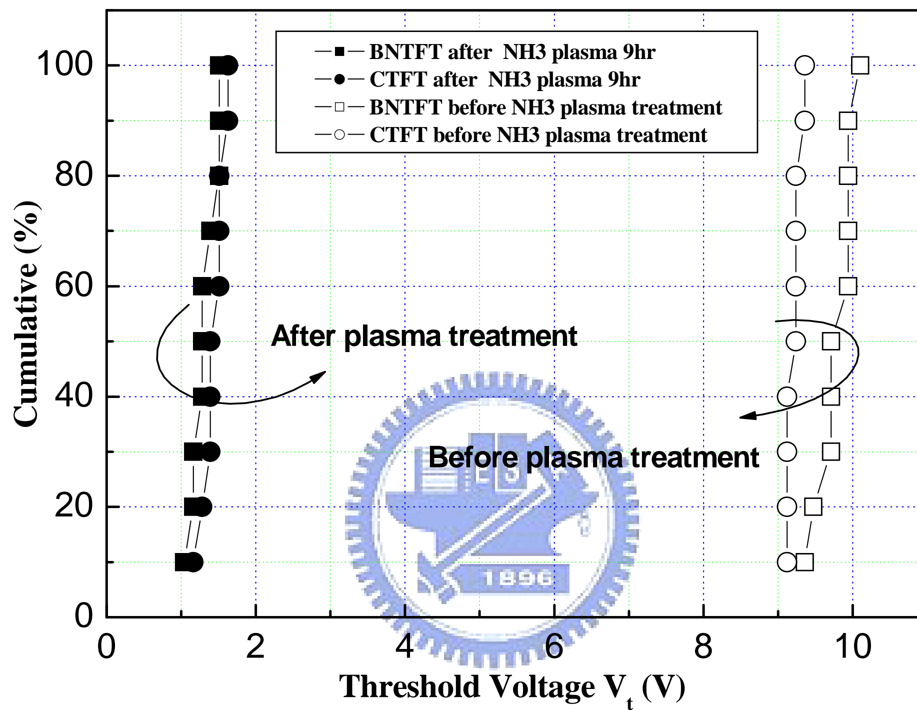

Figure 2.16 cumulative distribution of Threshold voltage before and after plasma treatment for CTFTs and BNTFTs.

.